Pacific Northwest
NATIONAL LABORATORY

PNNL-33028 Vol.2

Technical Reference on Hydrogen Compatibility of Acrylonitrile-Butadiene Rubber (NBR)

H-Mat Program Supported by DOE HFTO

July 2022

Kevin L. Simmons
Wenbin Kuang

U.S. DEPARTMENT OF ENERGY

Prepared for the U.S. Department of Energy
under Contract DE-AC05-76RL01830

DISCLAIMER

This report was prepared as an account of work sponsored by an agency of the United States Government. Neither the United States Government nor any agency thereof, nor Battelle Memorial Institute, nor any of their employees, makes **any warranty, express or implied, or assumes any legal liability or responsibility for the accuracy, completeness, or usefulness of any information, apparatus, product, or process disclosed, or represents that its use would not infringe privately owned rights**. Reference herein to any specific commercial product, process, or service by trade name, trademark, manufacturer, or otherwise does not necessarily constitute or imply its endorsement, recommendation, or favoring by the United States Government or any agency thereof, or Battelle Memorial Institute. The views and opinions of authors expressed herein do not necessarily state or reflect those of the United States Government or any agency thereof.

PACIFIC NORTHWEST NATIONAL LABORATORY
operated by
BATTELLE
for the
UNITED STATES DEPARTMENT OF ENERGY
under Contract DE-AC05-76RL01830

Printed in the United States of America

Available to DOE and DOE contractors from
the Office of Scientific and Technical Information,
P.O. Box 62, Oak Ridge, TN 37831-0062
www.osti.gov
ph: (865) 576-8401
fax: (865) 576-5728
email: reports@osti.gov

Available to the public from the National Technical Information Service
5301 Shawnee Rd., Alexandria, VA 22312
ph: (800) 553-NTIS (6847)
or (703) 605-6000
email: info@ntis.gov
Online ordering: http://www.ntis.gov

PNNL-33028 Vol.2

Technical Reference on Hydrogen Compatibility of Acrylonitrile-Butadiene Rubber (NBR)

H-Mat Program Supported by DOE HFTO

July 2022

Kevin L. Simmons
Wenbin Kuang

Prepared for
the U.S. Department of Energy
under Contract DE-AC05-76RL01830

Pacific Northwest National Laboratory
Richland, Washington 99354

Summary

This technical reference covers a comprehensive array of evaluations on hydrogen compatibility of a common elastomer material used for high pressure applications, acrylonitrile-butadiene rubber (NBR). This document focuses on detailing the experimental results obtained from three main aspects: transport properties, physical properties, and mechanical properties. Background information can be found in our introduction document. This document may be update and revised periodically in response to the needs of the technical community; up-to-date versions can be requested from the editors at the address given below. The success of this technical reference relies on feedback from the technical community; please forward your comments, suggestions, criticisms and relevant public-domain date to:

Pacific Northwest National Laboratory
Kevin L. Simmons
902 Battelle Boulevard
P.O. Box 999, MSIN K2-44
Richland, WA 99352.

Acknowledgments

This technical reference was prepared with financial support through the H-Mat program by the U.S. Department of Energy (USDOE), Office of Energy Efficiency and Renewable Energy (EERE), Hydrogen and Fuel Cells Technologies Office (HFTO) under Contract Number DE-AC05-76RL01830. We also acknowledge support from the Environmental Molecular Sciences Laboratory (EMSL). EMSL is a national scientific user facility sponsored by the DOE's Office of Science, Biological and Environmental Research program that is located at Pacific Northwest National Laboratory (PNNL). Sandia National Laboratories (SNL), Oak Ridge National Laboratory (ORNL) and Savannah River National Laboratory (SRNL) are actively supporting the H-Mat efforts as team members in this multi-lab program. Sandia National Laboratories is a multi-mission laboratory managed and operated by National Technology & Engineering Solutions of Sandia, LLC, a wholly owned subsidiary of Honeywell International Inc., for the U.S. Department of Energy's National Nuclear Security Administration under contract DE-NA0003525.

Acronyms and Abbreviations

DOE	Department of Energy
EERE	Office of Energy Efficiency and Renewable Energy
HFTO	Hydrogen and Fuel Cell Technologies Office
PNNL	Pacific Northwest National Laboratory
SNL	Sandia National Laboratories
ORNL	Oak Ridge National Laboratory
SRNL	Savannah River National Laboratory
NBR	Acrylonitrile-Butadiene Rubber
ACN	Acrylonitrile
CB	Carbon black
SC	Silica
ZnO	Zinc oxide
ASME	American Society of Mechanical Engineers
CSA	Canadian Standards Association
ANSI	American National Standards Institute
SI	International System of Units
TDA	Thermal Desorption Analysis
G.C.	Gas Chromatography
ASTM	American Society for Testing and Materials
DSC	Differential Scanning Calorimetry
TMA	Thermal Mechanical Analysis
DMA	Dynamic Mechanical Analysis
CoF	Coefficient of Friction
RDF/XDF	Rapid/Explosive Decompression Failure
Micro-CT	Microcomputed Tomography
TEM	Transmission Electron Microscopy
HeIM	Helium-ion Microscopy
HAADF	High Angle Annular Dark Field
STEM	Scanning Transmission Electron Microscopy
EDS	Energy Dispersive Spectroscopy
XRD	X-ray Diffraction
DOS	Dioctyl Sebacate

Contents

Summary ii
Acknowledgments iii
Acronyms and Abbreviations iv
1.0 Test Material 8
2.0 Transport Properties 10
3.0 Physical Properties 12
4.0 Mechanical Properties 13
5.0 Morphological Properties 16
6.0 References 21
Appendix A – Title A.1

Figures

Figure 1. Chemical formula of NBR.

Figure 2. TDA results of model NBR compounds.

Figure 3. Curving fitting of hydrogen content for NBR-nF-nP.

Figure 4. Storage modulus values of model NBR compounds before and after static exposure to 90 MPa hydrogen.

Figure 5. Compression set values of model NBR compounds before, after static exposure to 90 MPa hydrogen, and after pressure cycling with 90 MPa hydrogen.

Figure 6. XCT images of model NBR compounds.

Figure 7. HeIM images of NBR-nF-nP.

Figure 8. HeIM images of NBR-nF-P.

Figure 9. HeIM images of NBR-F-P.

Figure 10. HeIM images of NBR-F-nP.

Figure 11. TEM images of model NBR compounds.

Figure 12. XRD profiles for model NBR compounds (black line: as received; red line: after static exposure at 28 MPa).

Tables

Table 1. Overview of Model NBR Compounds.

Table 2. Hydrogen diffusion coefficient of model NBR compounds.

Table 3. Density Measurements of model NBR compounds.

Table 4. Glass transition temperature of model NBR compounds.

Table 5. Summary of friction and wear testing of model NBR compounds in ambient air and high-pressure hydrogen.

Table 6. XRD data analysis.

1.0 Test Material

This technical reference focuses on NBR to ensure a good depth of experimental evaluation and a discussion of the results. The model NBR compounds are formulated collaboratively by PNNL, Kyushu University (Japan), and Takaishi Industries (Japan) and exclusively produced by Takaishi Industries. There are six (6) compounds in this model set with differences in plasticizer, filler, or a combination thereof, as listed in Table 1.

Table 1. Overview of model NBR compounds

	NBR-nF-nP	NBR-nF-P	NBR-CB	NBR-SC	NBR-F-P	NBR-F-nP
Base Material	NBR (Nipol 1042*)	NBR (Nipol 1042*)	NBR (Nipol 1042*)	NBR (Nipol 1042*)	NBR (Nipol 1042*)	NBR (Nipol 1042*)
Features	No Filler No Plasticizer	No Filler Plasticizer	Carbon black No Plasticizer	Silica No Plasticizer	Carbon Black Silica Plasticizer	Carbon Black Silica No Plasticizer
Base Rubber	100	100	100	100	100	100
Stearic Acid	1	1	1	1	1	1
Zinc Oxide	5	5	5	5	5	5
Sulfur	1.5	1.5	1.5	1.5	1.5	1.5
MBTS [a]	1.5	1.5	1.5	1.5	1.5	1.5
TMTD [a]	0.5	0.5	0.5	0.5	0.5	0.5
DOS [b]	-	10	-	-	10	-
Carbon Black (N330)	-	-	25	-	23**	19**
Silica (Nipsil VN3)	-	-	-	30	28**	23**
Density	1.032	1.015	1.118	1.152	1.182	1.175
Hardness (IRHD)	51.0	43.4	66.0	66.1	65.8	68.7

*Nipol 1042 (Zeon Corporation): Medium High Nitrile Rubber, Acrylonitrile content 33.5%
**Hardness of NBR-F-P and NBR-F-nP is set at A 70 by filler content as shown in the table. The ratio of carbon black and silica is 25/30.
[a] Accelerators – MBTS:2,2'-benzothiazyl disulfide, TMTD: bis(dimethylthiocarbamoyl) disulfide
[b] Plasticizer – DOS: dioctyl sebacate

The most common NBR (chemical formula shown in Figure 1) compounds come with standard acrylonitrile (ACN) content of 34%. However, the ACN content can be varied from 15% to 50% to adjust the thermal characteristics and chemical resistance properties (e.g., swelling resistance) of the material depending on the application. In general, the rule of thumb is that high ACN contents result in low volume swell and poor low-temperature flexibility, and vice versa. [1] Also, researchers reported that glass transition temperature and decomposition temperature would decrease with increasing the ACN content. [2] This is because the ACN contents have a significant influence on the thermal characteristics of NBR compounds due to the ability to restrict the mobility of the polymer chain and lead to a higher decomposition temperature than the butadiene portion.

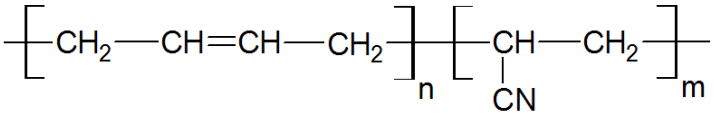


Figure 1. Chemical formula of NBR.

2.0 Transport Properties

In practice, to estimate the diffusion coefficient for hydrogen in the model NBR compounds, an arbitrary diffusion coefficient value is assigned to the equation provided above to calculate the corresponding hydrogen concentration profile, which is subsequently used to compare with the experimental data. Based on the difference between the calculated curve and the experiments-derived data, a new diffusion coefficient value is generated to minimize that difference. The process is repeated until the two curves overlap each other. Then, the equilibrium hydrogen concentration can be obtained from the equation, and a derivative of the curve is created to obtain the diffusion coefficient. In our tests, rubber composites were exposed to 27.6 MPa hydrogen pressure at room temperature for 24 h, followed by decompression at 30°C under argon flow (50 mL/min).

The test results are plotted on both a log basis and a linear basis in Figure 4. Initial curve fits using the equation provided above and a single value of D were unsatisfactory; as a result, all experimental release profiles were fit using a linear combination of two release curves, $C_{t,1}$ and $C_{t,2}$, representing the rubber polymer and fillers separately, as illustrated in Figure 5. The plasticizer and the filler (carbon black) had a significant effect on C_0 in each rubber composite; the plasticizer decreased the hydrogen content and increased the diffusion coefficient, while the the filler increased the hydrogen content and decreased the diffusion coefficient. The hydrogen diffusion coefficients are summarized in Table 2.

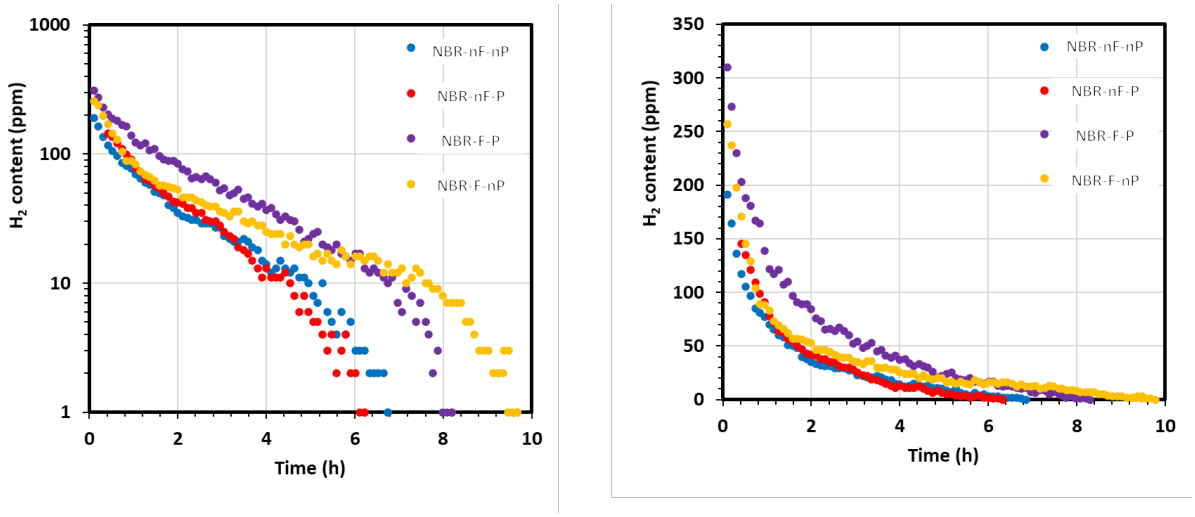


Figure 2. TDA results of model NBR compounds after 27.6 MPa exposure.

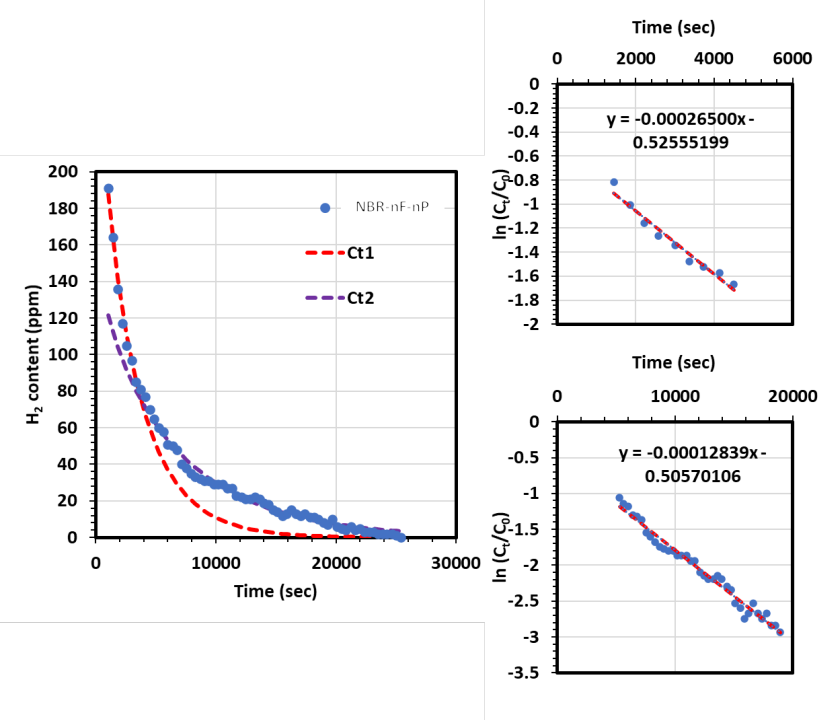


Figure 3. Curving fitting of hydrogen content for NBR-nF-nP.

Table 2. Hydrogen diffusion coefficient of model NBR compounds after 27.6 MPA exposure

	Thickness (mm)	Radius (mm)	C_0 (ppm)	D1 (m^2/s)	D2 (m^2/s)
NBR-nF-nP	2.93	5.86	464	1.954×10^{-10}	9.467×10^{-11}
NBR-nF-P	2.92	5.88	845	2.000×10^{-10}	1.260×10^{-10}
NBR-F-P	2.77	5.61	771	1.908×10^{-10}	8.895×10^{-11}
NBR-F-nP	2.93	5.86	464	2.503×10^{-10}	5.641×10^{-11}

3.0 Physical Properties

The density measurements of model NBR compounds before, immediately after exposure to 90 MPa hydrogen, 48 hours after, and after pressure cycling between 17 MPa and 87 MPa in hydrogen for 100 times are summarized in Table 3.

Table 3. Density Measurements of model NBR compounds

	Before 90 MPa H_2 (g/cm^3)	Immediately after 90 MPa H_2 (g/cm^3)	48 hours after 90 MPa H_2 (g/cm^3)	Pressure cycling with 87 MPa H_2 (g/cm^3)
NBR-nF-nP	1.017±0.012	0.569±0.036	1.023±0.008	0.718±0.010
NBR-nF-P	0.999±0.003	0.539±0.005	1.026±0.024	0.930±0.058
NBR-F-P	1.167±0.013	0.680±0.020	1.201±0.013	0.811±0.005
NBR-F-nP	1.186±0.002	0.766±0.025	1.170±0.006	0.893±0.007

We found a noticeable decrease (>35%) in density for four model NBRs immediately after exposure. This phenomenon is primarily attributed to the volume increase caused by the limited diffusion rate of hydrogen within the polymer upon removal of the external pressure. Then, all samples regained the density lost within 48 hours after hydrogen exposure, which suggests that the hydrogen trapped in the polymer had escaped almost completely. However, we observed up to a 30% permanent decrease in density across all compounds after the 100 pressure cycles of hydrogen exposure, indicative of significant volumetric expansion and internal material damage.

The glass transition temperatures of four model NBR compounds before hydrogen exposure, immediately after static exposure, and after pressure cycling is listed in Table 4. No significant changes in the glass transition temperature of model NBR compounds were observed before and after static exposure to 90MPa hydrogen.

Table 4. Glass transition temperature of model NBR compounds before and after exposure

	Before 90 MPa H_2 (°C)	After 90 MPa H_2 (°C)
NBR-nF-nP	-7.9±1.1	-9.3±0.9
NBR-nF-P	-15.9±0.3	-15.5±0.5
NBR-F-P	-16.0±0.4	-15.6±0.3
NBR-F-nP	-8.7±0.2	-8.2±0.4

4.0 Mechanical Properties

The modulus results of model NBR compounds before and after static exposure to 90 MPa hydrogen are compiled in Figure 4. Note that all storage modulus and loss modulus values are compared at 25°C. A frequency of 1 Hz and a temperature ramp rate of 5°C/min is used for the testing. The post-exposure data points are taken 48 hours after the specimens are removed from the pressure vessel. The results indicated no significant changes in storage modulus at 25 °C for all model NBR compounds after exposure to 90MPa hydrogen.

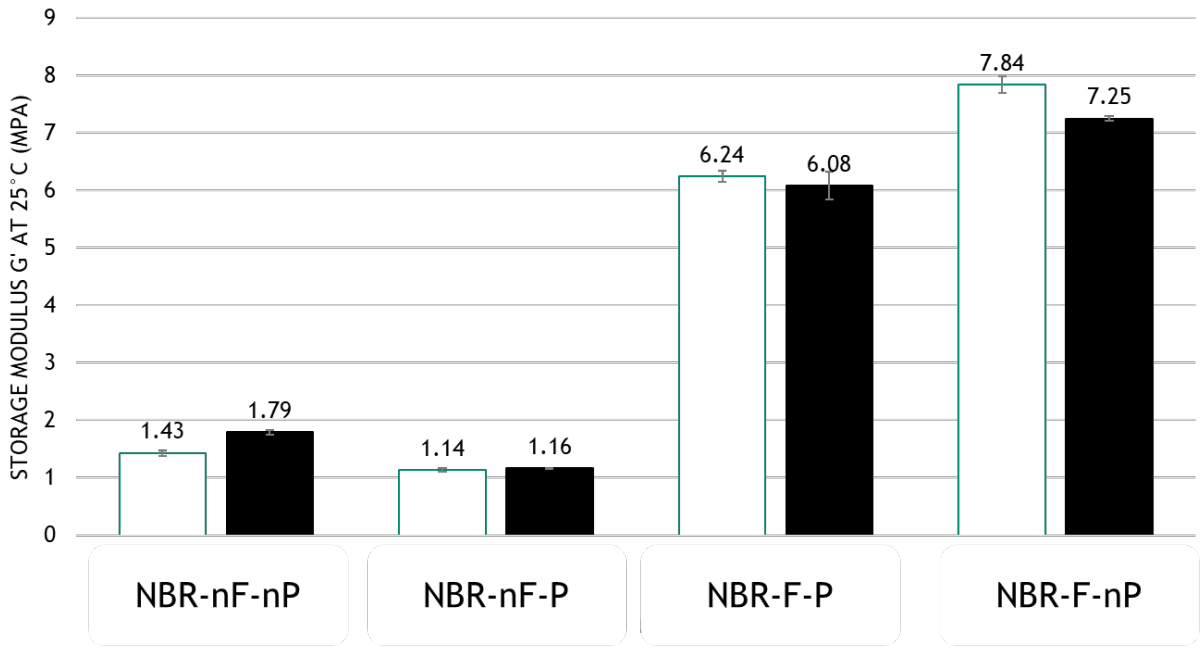


Figure 4. Storage modulus values of model NBR compounds before and after static exposure to 90 MPa hydrogen. Hollow bar = before static exposure; solid bar = after static exposure.

The results of compression set measurements are plotted in Figure 5. The hollow bars represent the data obtained before hydrogen exposure. The solid bars represent the data collected after static exposure to 90 MPa hydrogen. The hatch angled bars represent the data for the specimens that are pressure cycled with 90 MPa hydrogen. Note that the specimens were compressed to 75% for 22 hours at 110°C and allowed 30 min for recovery prior to measuring the compression set. The results indicated that the addition of plasticizer (i.e., DOS) caused an increase in compression set after hydrogen exposure, as NBR-nF-P and NBR-F-P showed a 65.8% and 36.6% increase, respectively. The NBR-nF-nP and NBR-F-nP compression set after hydrogen exposure indicated a change of less than 19%. Since our prior study [3] confirmed that plasticizer migrates and concentrates when subject to hydrogen exposure, we attributed such changes in compression set to a combinational effect of the hydrogen-provoked plasticizer migration and the hydrogen dissolved within polymer, causing increased change slippage and increased volume swell after decompression. After 100 pressure cycles, all compounds were found to have a modest decrease in compression set

values. This is likely due to the hydrogen degradation effects that are likely caused by accumulation of numerous micro-voids throughout multiple rapid decompression processes and loss of filler bonding. Both filled compunds (i.e., NBR-F-P and NBR-F-nP) presented a ≤10% average drop while compression set was shown to be higher for (27% for NBR-nF-nP and 13% for NBR-nF-P) values in the unfilled systems after the pressure cycling. Such different behavior was ascribed to the fact that the fillers can reinforce the matrix polymer and mitigate crack initiation to some extent.

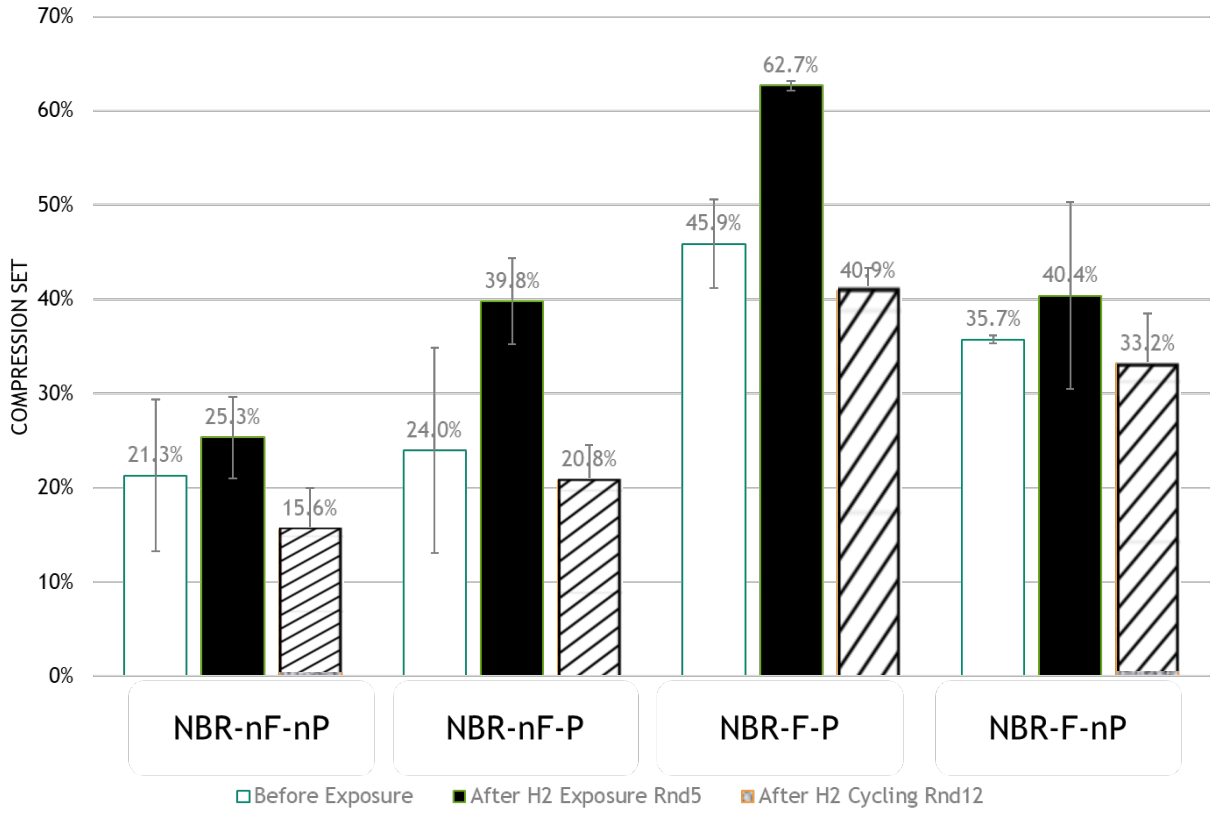


Figure 5. Compression set values of model NBR compounds before, after static exposure to 90 MPa hydrogen, and after pressure cycling with 90 MPa hydrogen. Hollow bar = before static exposure; solid bar = after static exposure; angled hatch = after cycling.

The results from friction and wear testing are summarized in Table 5. The introduction of high-pressure hydrogen led to an increase in CoF for all of the model compounds. The effects of blended plasticizer and/or fillers on the tribological performance were discussed comparatively in terms of the CoF and wear factor, revealing that the presence of the plasticizer results in relatively low wear in both environments due to its lubricating nature. Reduced wear was observed on almost all the model compounds that were exposed to hydrogen; however, the NBR-F-nP's wear factor increased dramatically in high-pressure hydrogen because of hydrogen-induced surface morphology alteration. We postulate that such surface morphology alteration becomes independent of hydrogen exposure time once 100% saturation is achieved since most of the relevant literature [4-7] concludes that hydrogen-polymer interaction is basically physical. Also, optical profilometry (Bruker Contour GT-I) is performed to measure root mean square roughness (Sq) within a sample area of 2.5 × 1.9 mm2. Average amplitude in the

height direction and corresponding roughness contour map is obtained within the scanned area. Bruker's Vision64 software is used for data analysis.

Table 5. Summary of friction and wear testing of model NBR compounds in ambient air and high-pressure hydrogen

	NBR-nF-nP	NBR-nF-P	NBR-F-P	NBR-F-nP
COF_{air}	1.455±0.021	0.875±0.026	0.613±0.011	0.742±0.010
COF_{H2}	2.209±0.030	1.379±0.004	1.031±0.008	1.955±0.013
ΔCOF (%) [a]	+51.8%	+57.6%	+68.2%	+163.5%
K_{air} (mm×10^{-6}/(MPa*mm/s^{-2}))	0.179±0.023	0.280±0.048	0.389±0.049	0.335±0.036
K_{H2} (mm×10^{-6}/(MPa*mm/s^{-2}))	0.150±0.019	0.105±0.006	0.076±0.030	0.848±0.079
ΔK (%) [a]	-16.2%	-62.5%	-80.5%	+153.1%
S_q [b]	0.568±0.137	0.523±0.134	0.966±0.228	0.498±0.121
$S_{q,H2}$ [c]	0.586±0.051	0.572±0.097	0.528±0.088	0.448±0.065
ΔS_q (%)	+3.2%	+9.4%	-45.3%	-10.0%

[a] Calculation based on increase relative to air condition
[b] Averaged root mean square roughness from an area of 1.9 mm × 2.5 mm (S_q). Tested before hydrogen exposure and no wear testing performed
[c] Tested after hydrogen exposure and no wear testing performed

5.0 Morphological Properties

The XCT images of model NBR compounds before and after static exposure to 90 MPa hydrogen are shown in Figure 6. In particular, the damage formed in the unfilled, unplasticized system (NBR-nF-nP) post-exposure mostly take the form of slits and cracks with a small fraction being round voids. When plasticizer is added to the rubber (both NBR-nF-P and NBR-F-P), round voids became the predominant form of damage with a significantly increased quantity. We postulate that the added plasticizer results in lower density and more free volume space for hydrogen to concentrate, given the different solubility of hydrogen in plasticizer within the polymer. Research [3] has found that the shrinkage in free volume caused by hydrostatic effects of hydrogen gas pressure decreases diffusion coefficient, resulting in the decrease of permeability coefficient with the pressure rise. This is shown by an increase in the loss in density seen in plasticized compounds compared to their unplasticized counterparts immediately after static exposure. For NBR-F-nP, the presence of fillers and lack of plasticizer resulted in a reduction in voids through static exposure to high-pressure hydrogen gas. In addition, the voids formed were generally small-to-medium sized. We concluded that the damage mitigation by fillers is quite effective at the micrometer scale while plasticizer significantly undermines it when present.

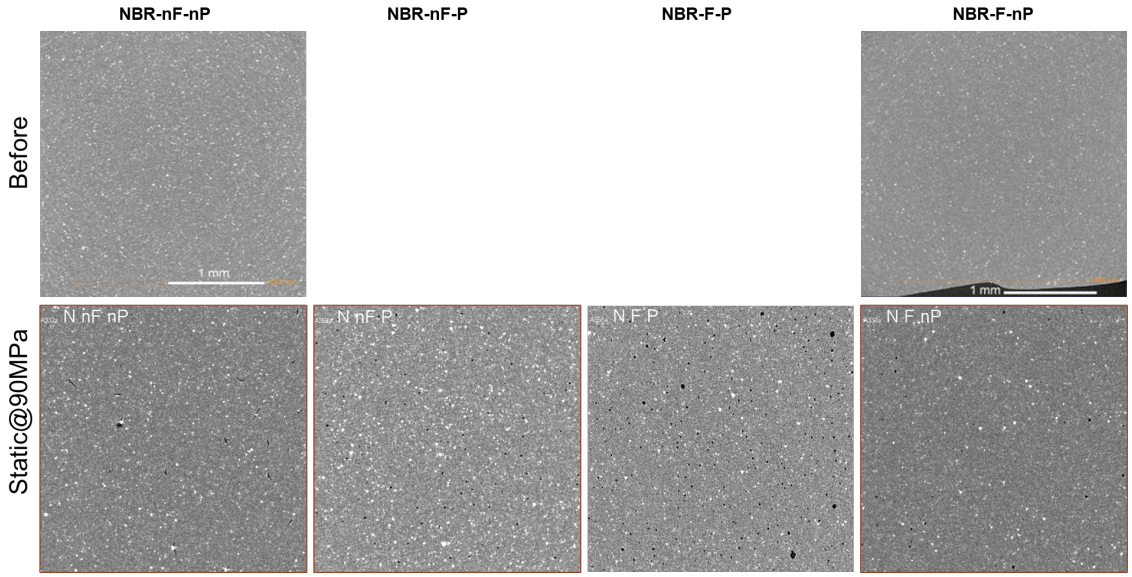


Figure 6. XCT images of model NBR compounds.

None of the unplasticized rubber compounds (i.e., NBR-nF-nP and NBR-F-nP) showed noticeable morphological alteration after static or cyclic exposure at this small length scale. However, NBR-nF-P and NBR-F-P experienced a heavy migration and coalescing of the dioctyl sebacate (DOS) plasticizer shown by forming dark spots in the statically exposed samples or larger dark regions in the cyclically exposed samples. This migration and phase separation was validated by the time-of-flight secondary ion mass spectrometry (TOF-SIMS) results published previously [8]. This observation aligns well with the micro-CT results, indicating the hydrogen effects on material morphology and consequentially damage formation.

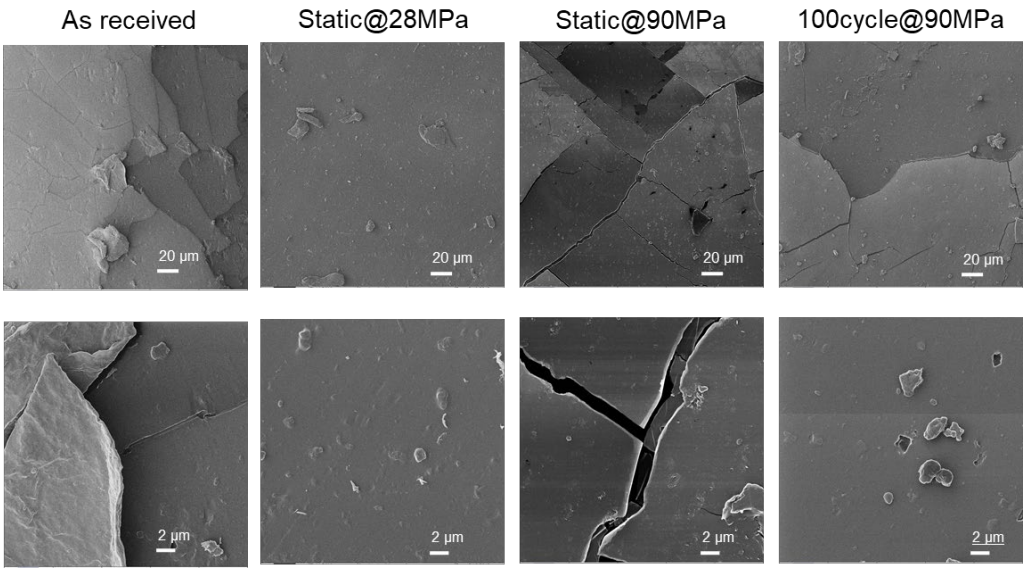


Figure 7. HeIM images of NBR-nF-nP.

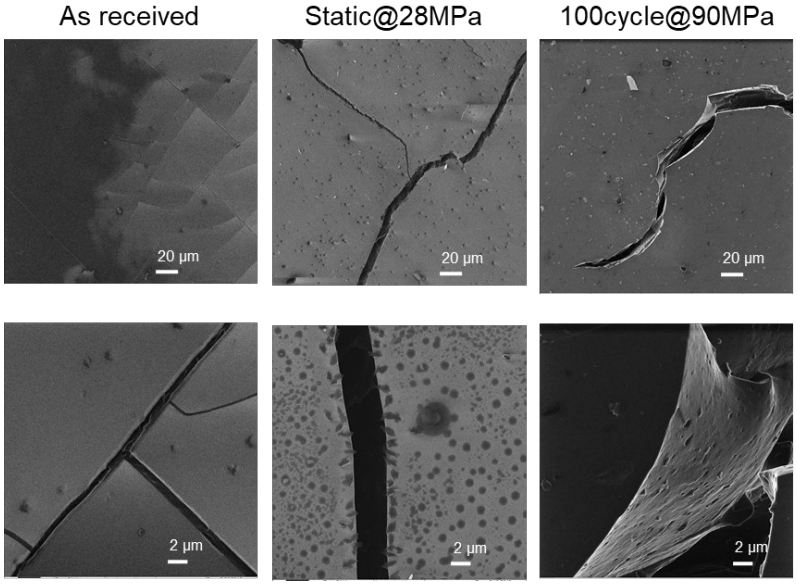


Figure 8. HeIM images of NBR-nF-P.

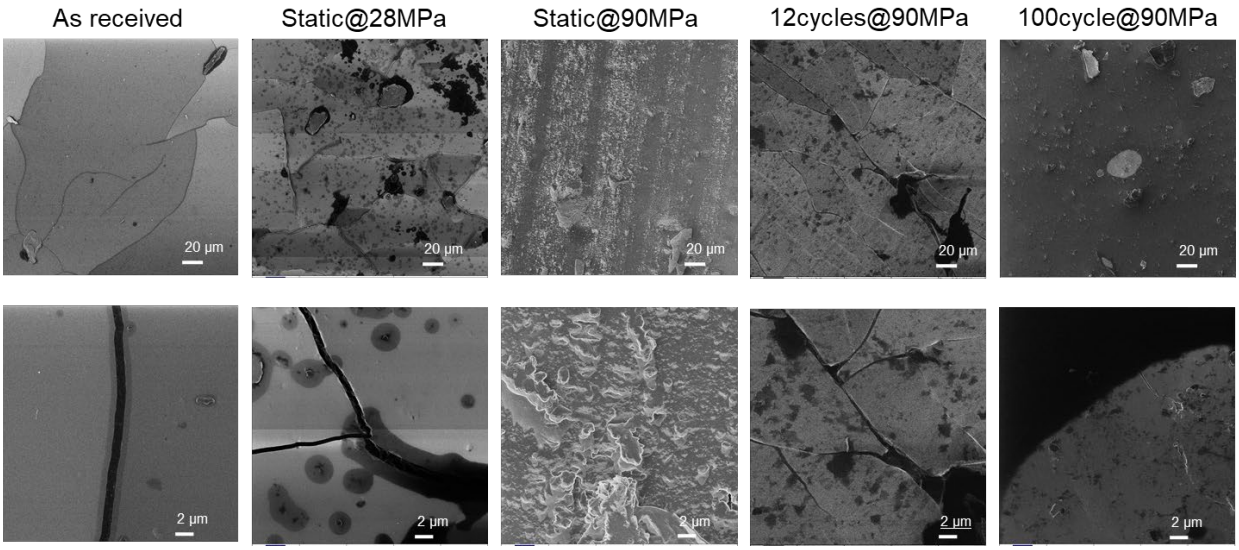


Figure 9. HeIM images of NBR-F-P.

NBR-F-P is a filled, plasticized system that simulates the recipe of a commercial elastomer for high-pressure applications. Major morphological changes occurred under all hydrogen conditions in this study. These changes in the material mainly include surface cracking and plasticizer migration. The impacts of these changes could lead to increased long-term damage and eventual collapse of structural integrity of the material. The latter could cause local property changes and alteration of rubbery characteristics, which are important factors in determining sealing performance.

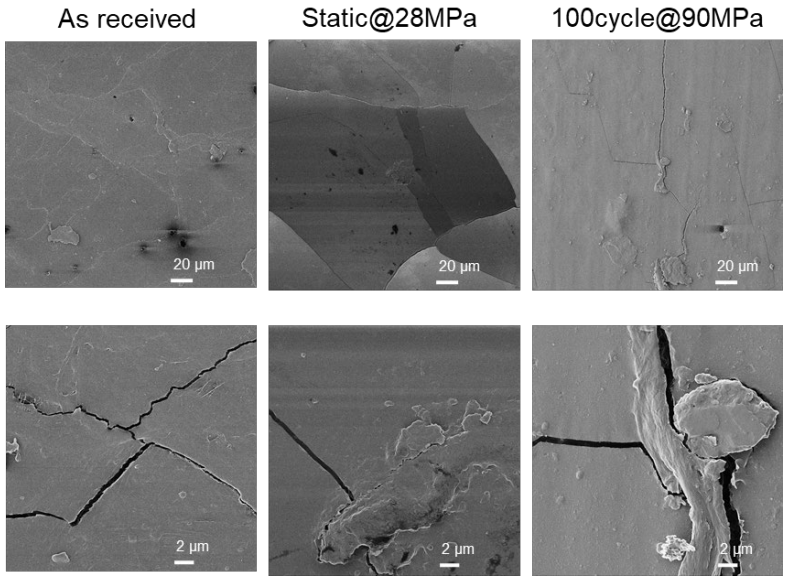


Figure 10. HeIM images of NBR-F-nP.

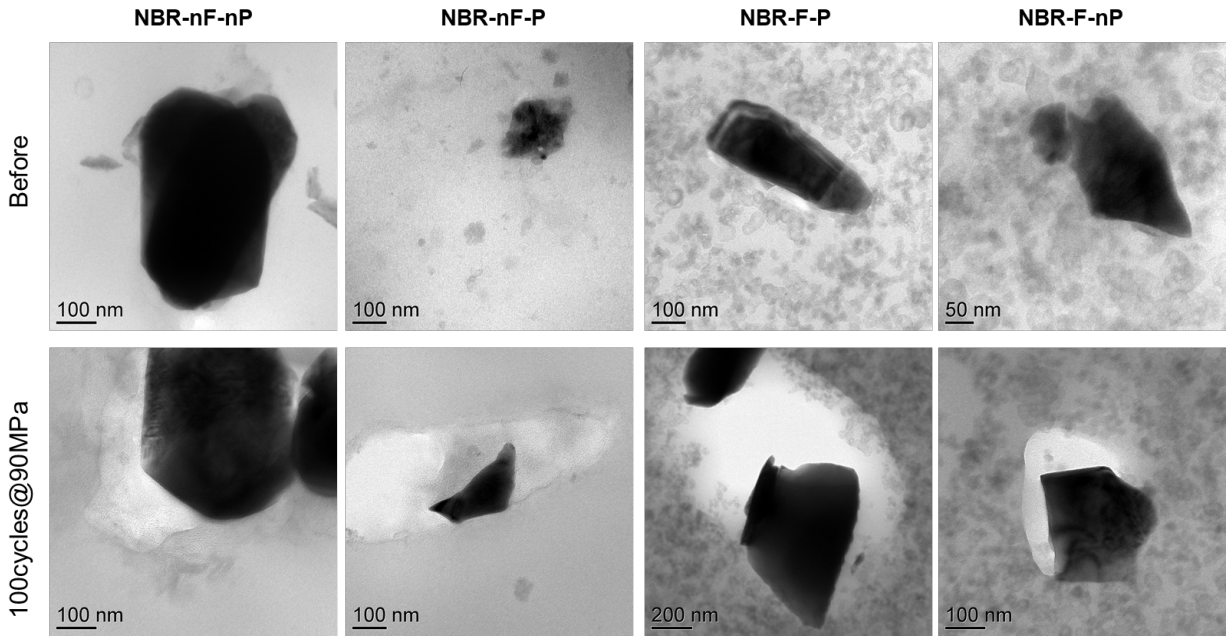


Figure 11. TEM images of model NBR compounds.

Microtome has been widely used in the science community as an advanced cutting tool to prepare extremely thin slices of material for observation under transmitted light or electron radiation. NBR-nF-P and NBR-F-P are sectioned into slices about 70 nm thick which were subsequently mounted on copper grids for imaging. Figure 11 shows the change in internal morphology of these two rubber compounds before and after pressure cycling with 90 MPa hydrogen gas. Interestingly, a gray "halo" structure is found appearing around the zinc oxide particles (dark particles shown in the images) in NBR-nF-P after hydrogen exposure. This could be evidence of interfacial detachment between zinc oxide particles and polymer matrix caused by hydrogen. Additionally, there is an increase in smaller zinc oxide particles (<30 nm) in the exposed sample than in the as-received sample. In contrast, we observe that smaller filler particles of carbon black and silica in NBR-F-P become less uniformly distributed after exposure to hydrogen, leaving many filler-lacking regions. We speculate that it relates, if not all, to larger filler-polymer detaching at the interface, and this could affect hydrogen diffusion behavior.X-ray diffraction (XRD) is a non-destructive test method used to identify the crystalline phases present in a material. Zinc oxide typically exists in the form of crystals, so XRD can be used to study any structural change to zinc oxide and surrounding matrix material as TEM suggested significant alteration in morphology around surface of the zinc oxide after hydrogen exposure. Figure 12 shows XRD patterns for all four NBR compounds, and we observed no major change in chemical structure as the patterns are identical before and after hydrogen exposure. Bragg's law is used to estimate the crystal size of zinc oxide particles and the results are summarized in Table 6. The zinc oxide particle decreases in size, after exposure to 28 MPa hydrogen, for all model compounds except NBR-nF-nP. This agrees with our TEM observations where the quantity of smaller zinc oxide particles increased after the hydrogen treatment.

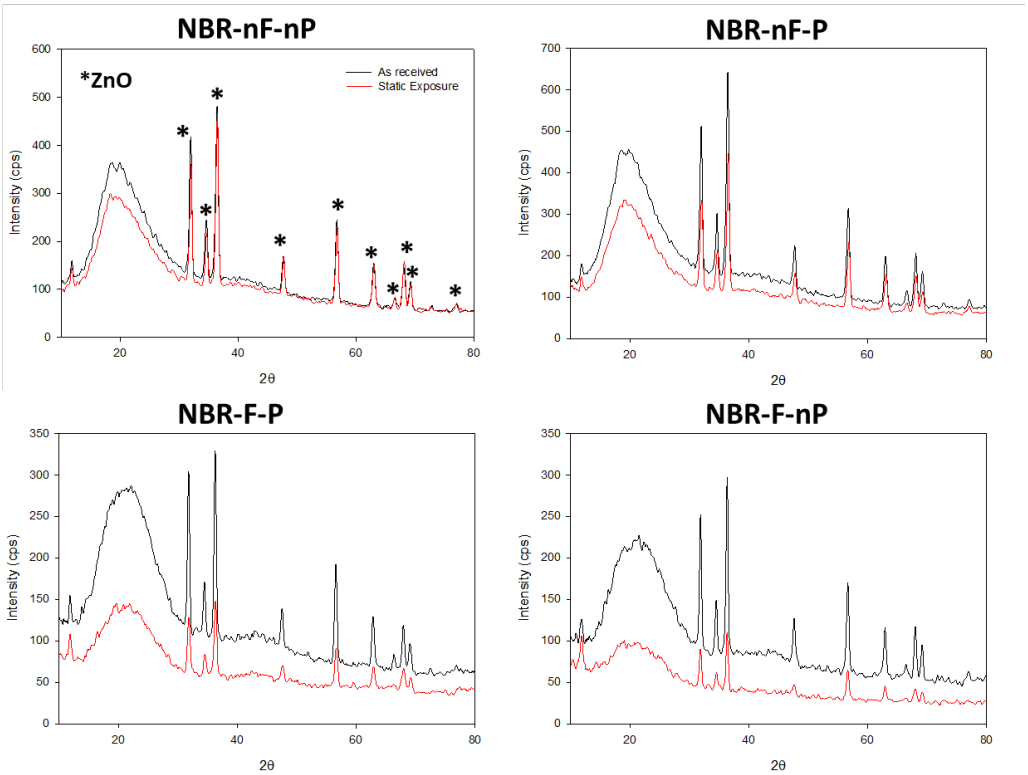


Figure 12. XRD profiles for model NBR compounds (black line: as received; red line: after static exposure at 28 MPa).

Table 6. XRD data analysis

	ZnO size (nm)	d spacing (Å) at 2θ ~20
NBR-nF-nP (as received)	19.9	4.611
NBR-nF-nP (static exposure)	34.8	4.604
NBR-nF-P (as received)	30	4.637
NBR-nF-P (static exposure)	21.7	4.604
NBR-F-P (as received)	35.1	4.203
NBR-F-P (static exposure)	22.6	4.137
NBR-F-nP (as received)	38	4.205
NBR-F-nP (static exposure)	30.7	4.275

6.0 References

1. Choi, S, Ha S. Influence of the swelling temperature and acrylonitrile content of NBR on the water swelling behaviors of silica-filled NBR vulcanizates. Journal of Industrial and Engineering Chemistry. 2009, Volume 15, Issue 2, Pages 167-170, https://doi.org/10.1016/j.jiec.2008.09.016.
2. Lee YS, Ha K. Effects of acrylonitrile content on thermal characteristics and thermal aging properties of carbon black-filled NBR composite. Journal of Elastomers & Plastics. 2021;53(5):402-416. doi:10.1177/0095244320941243.
3. Fujiwara, Hirotada, et al. "Hydrogen permeation under high pressure conditions and the destruction of exposed polyethylene-property of polymeric materials for high-pressure hydrogen devices (2)-." International Journal of Hydrogen Energy 46.21 (2021): 11832-11848.
4. Yamabe, J. and Nishimura, S. (2011), "Influence of Carbon Black on Decompression Failure and Hydrogen Permeation Properties of Filled Ethylene-Propylene-Diene-Methylene Rubbers Exposed to High-Pressure Hydrogen Gas," Journal of Applied Polymer Science, 122(5), pp 3172-3187.
5. Yamabe, Junichiro, Takashi Matsumoto, and Shin Nishimura. "Application of acoustic emission method to detection of internal fracture of sealing rubber material by high-pressure hydrogen decompression." *Polymer testing* 30.1 (2011): 76-85.
6. Ohyama, Keiko, Hirotada Fujiwara, and Shin Nishimura. "Inhomogeneity in acrylonitrile butadiene rubber during hydrogen elimination investigated by small-angle X-ray scattering." *International Journal of Hydrogen Energy* 43.2 (2018): 1012-1024.
7. Castagnet, Sylvie, et al. "In-situ X-ray computed tomography of decompression failure in a rubber exposed to high-pressure gas." *Polymer Testing* 70 (2018): 255-262.
8. Simmons, Kevin L., Wenbin Kuang, Sarah D. Burton, Bruce W. Arey, Yongsoon Shin, Nalini C. Menon, and D. B. Smith. "H-Mat hydrogen compatibility of polymers and elastomers." International Journal of Hydrogen Energy 46, no. 23 (2021): 12300-12310.

Appendix A – Title

Use Body Text for paragraphs in this section. PNNL reports use http://www.chicagomanualofstyle.org/home.html for document style. Right-click and choose open hyperlink to view the style guide.

Pacific Northwest National Laboratory

902 Battelle Boulevard
P.O. Box 999
Richland, WA 99354
1-888-375-PNNL (7665)

www.pnnl.gov